Analytical Methods

ROYAL SOCIETY OF CHEMISTRY

PAPER

View Article Online
View Journal | View Issue

Cite this: *Anal. Methods*, 2021, **13**, 2021

Femtomolar determination of an ovarian cancer biomarker (miR-200a) in blood plasma using a label free electrochemical biosensor based on L-cysteine functionalized ZnS quantum dots†

Mahboobe Moazampour, Hamid R. Zare * and Zahra Shekari

Received 25th February 2021
Accepted 22nd March 2021

DOI: 10.1039/d1ay00330e

rsc.li/methods

In the present study, a label-free electrochemical genosensor was designed based on ZnS quantum dots functionalized with L-cysteine (Cys–ZnS-QDs) to detect miR-200a, as a special ovarian cancer biomarker. The Cys–ZnS-QD genosensor was characterized by transmission electron microscopy (TEM), UV-Vis absorption and fluorescence methods. Cys–ZnS-QDs are electrodeposited on the glassy carbon electrode surface and act as a suitable substrate for immobilization of the DNA probe. The effective parameters in the preparation of the genosensor are optimized to improve its analytical performance. The analytical performance of the genosensor has been investigated using electrochemical impedance spectroscopy. Under optimal conditions, the linear range and the detection limit of miR-200a were found to be 1.0×10^{-14} to 1.0×10^{-6} M and 8.4 fM. In addition, the genosensor is used to detect the target complementary miRNA strand from a single-base mismatch miRNA strand. Finally, this label-free electrochemical biosensor was used to detect miR-200a in human plasma without using any amplification method.

1. Introduction

MicroRNAs (miRNAs) are an important class of short, single-stranded and nonprotein encoding single-stranded ribonucleic acids (RNA) that play an important role in gene expression by binding to target messenger RNAs (mRNAs).[1,2] To date, more than 2500 miRNAs have been identified and research shows that miRNAs are associated with many diseases, including tumor metastasis, neurological diseases, and a variety of human cancers.[3,4] Circulating miRNAs are stable in the blood, allowing us to identify distant tumors in liquid biopsies.[5] These circulating miRNAs can be employed as a biomarker for cancer diagnosis.[1] Cancer is currently one of the most important public health problems in the world, and cancer generally involves uncontrolled and abnormal growth of the cells.[6] Ovarian cancer is the fifth most common cause of cancer deaths in women in the western world, most of which are due to late diagnosis.[7] Ovarian cancer is more difficult to treat than other cancers in women, with the mortality rates among all cancer types being estimated at 5%, while the survival rate for ovarian cancer is 40%.[8] Research shows that the expression profiles of the miRNA-200 family (miR-200a, miR-200b, and miR-200c) play an important role in the diagnosis of ovarian cancer. In the miRNA-200 family, miR-200a is about five times higher in the first and second stages (early stage of cancer) and 8 times higher in the third and fourth stages (advanced stages of cancer) than in the blood of a healthy person.[4,9] Measurements and comparison of miR-200a levels in normal and patient samples have been investigated in some studies. In one of these studies, the relative quantitative real-time polymerase chain reaction (qPCR) was used to measure the expression of miR-200a. Data analysis was also performed using a comparative threshold cycle method to calculate the normalized miRNA level. In this study, normalized miRNA levels for normal and cancerous samples were reported to be −16.2 and −21.1, respectively. In addition, the mean fold-change of miR-200a expression in cancer samples relative to normal samples was reported to be 18.6-fold.[10] In another study, the mean expression of miR-200a in cancer samples compared to normal samples was reported to be 6.04.[11]

On the other hand, a very sensitive technique is needed to detect miRNAs because the concentration of miRNAs is very low.[12] Up to now, various techniques such as quantitative reverse transcription-polymerase chain reaction (qRT-PCR),[13] microarrays,[14] and flowcytometry[15] have been reported for miRNA detection. Despite their advantages, these methods have disadvantages such as the need for expensive reagents, time-consuming analysis, and low reproducibility.[16] One of the best ways to detect miRNAs is to use electrochemical biosensors

Department of Chemistry, Faculty of Science, Yazd University, Yazd, 89195-741, Iran. E-mail: hrzare@yazd.ac.ir; Fax: +98 35 38210991; Tel: +98 35 31232669

† Electronic supplementary information (ESI) available. See DOI: 10.1039/d1ay00330e

because they are simple, inexpensive, portable and highly sensitive.[16] A key step in the design of electrochemical biosensors is the immobilization of biomolecules on the surface of a sensor and the formation of an electron transfer mediator between the biological materials and the electrode surface.[17] In addition, nanomaterials are used in the manufacture of biosensors to increase the sensitivity, surface stability and effective immobilization of biological materials on the electrode surface.[18–24] Quantum dots are semiconductor nanocrystals with very small size and specific electrical properties. Quantum dots are used in the production of biosensors due to their good electrochemical properties and easy synthesis.[25,26] The small particle size of quantum dots provides more sites for bioreceptors to be trapped on the surface of the substrate. For this reason, these nanomaterials are widely used in the design of electrochemical biosensors. Metal sulfide quantum dots, such as ZnS quantum dots (ZnS-QDs), are used in biology and medicine to track, measure, image, and diagnose cancer. ZnS is a semiconductor with good biocompatibility.[27,28] By activation, the ZnS-QD surface with appropriate functional groups and substrates with low toxicity and high efficiency can be prepared for stabilization of biological materials. In addition, stabilization of compounds with functional groups on the ZnS-QD surface results in the production of water-soluble and environmentally friendly compounds. Compounds with functional groups stabilized on the surface of ZnS-QDs are also used to bind different biomaterials to the surface of quantum dots.[29,30]

Electrochemical impedance spectroscopy (EIS) is one of the most effective methods for measuring interfacial properties in the biomolecular recognition events at the modified electrode surface. EIS is a non-destructive technique and it has high sensitivity.[31,32] EIS can be performed in the presence or absence of a redox pair, called faradaic EIS and non-faradaic EIS, respectively.

In the present research, ZnS quantum dots (ZnS-QDs) were functionalized with L-cysteine (Cys). L-Cysteine has different functional groups. These functional groups allow the probe to be immobilized on the electrode surface. The small size of the ZnS-QDs creates more sites for the probes to attach on the electrode surface, thus increasing sensitivity. To the best of our knowledge, no studies have been performed using Cys–ZnS-QDs to fabricate miR-200a genosensors. In this study, electrochemical impedance spectroscopy (EIS) was used to confirm the immobilization of the miRNAs at the modified electrode surface. A wide linear concentration range and low detection limit were obtained for measuring miR-200a without using any label by the EIS method. This label-free genosensor was also used to detect and discriminate the target complementary DNA from non-complementary and mismatch oligonucleotides.

2. Experimental

2.1 Reagents, apparatus and electrochemical measurements

Analytical grade reagents including zinc acetate dihydrate ($Zn(OAc)_2 \cdot 2H_2O$), sodium sulfide ($Na_2S \cdot 9H_2O$), sodium hydroxide, L-cysteine (Cys), *N*-(3-dimethylaminopropyl)-*N*′-ethyl carbodiimide hydrochloride (EDC), *N*-hydroxysuccinimide (NHS), potassium ferricyanide, potassium ferrocyanide, and other chemical reagents were obtained from Merck Company. Double distilled water was used to prepare all the experimental solutions, and oligonucleotide solutions were prepared with ultra-pure water. All the oligonucleotides were purchased from Bioneer Corporation (South Korea). The stock solutions of the oligonucleotides (100.0 μM) were prepared with 10.0 mM Tris–HCl buffer (pH 8.0) containing 1.0 mM EDTA. The immobilization solution was 1.0 M phosphate buffer (pH 4.5), and the hybridization and washing solutions were 0.05 M phosphate buffer (pH 7.0) containing 0.3 M NaCl. The stock solutions of all the oligonucleotides were kept at −20 °C. 0.1 M phosphate buffer (pH 7.0) containing 5.0 mM $K_3[Fe(CN)_6]$, and 5.0 mM $K_4[Fe(CN)_6]$ in a 1 : 1 ratio and 0.1 M KCl was used for the electrochemical impedance spectroscopy (EIS) experiments.

MiR-200a was selected as a biomarker of ovarian cancer and complementary sequence. A single strand of DNA with similar sequences was used instead of RNA as a complementary sequence to solve the problems of working with RNA, for example, low stability and folded structures. In fact, U bases of the miR-200a sequence have been replaced with T bases in the complementary sequence. The corresponding oligonucleotides sequences are listed below:

NH_2-probe sequence: 5′-NH_2-TCC AGC ACT GTC CGG TAA GAT G-3′

Complementary (miR-200a) sequence: 5′-CAT CTT ACC GGA CAG TGC TGG A-3′

Single-base mismatch sequence: 5′-CAT CGT ACC GGA CAG TGC TGG A-3′

Non-complementary (miR-25) sequence: 5′-CAT TGC ACT TGT CTC GGT CTG A-3′

Healthy human plasma was obtained from a local clinical laboratory (Sina Pathobiology Laboratory, Yazd, Iran) and stored at −20 °C. Ethical considerations of this study have been approved by the General Research Ethics Committee of Faculty of Chemistry, Yazd University, with the ethical code 30/353.

All electrochemical experiments were performed with an Autolab potentiostat/galvanostat model PGSTAT 30 (Eco-Chemic, Utrecht, Netherlands) at room temperature in an enclosed Faraday cage. A three-electrode system consisting of a modified glassy carbon working electrode, a platinum auxiliary electrode and an Ag/AgCl/KCl (sat'd) reference electrode was also used (Azar Electrode Co, Iran). The pH measurements were performed with a Metrohm model 827 pH /mV meter. The morphology and particle size of the prepared Cys–ZnS-QDs were determined by transmission electron microscopy (TEM) (Philips-CM300, Netherlands). Optical spectra of Cys–ZnS-QDs were obtained by using a UV-Vis spectrophotometer (model SPECORD 250 Analytik Jena AG, Germany) and fluorescence array (model FL-Ar, Iran). The EIS measurements were performed in the frequency range of 10 mHz to 100 kHz with an amplitude of 10 mV and applied potential of 0.25 V. The EIS data were fitted to a Randles equivalent circuit by using Nova software from Autolab and shown in the Nyquist plots.

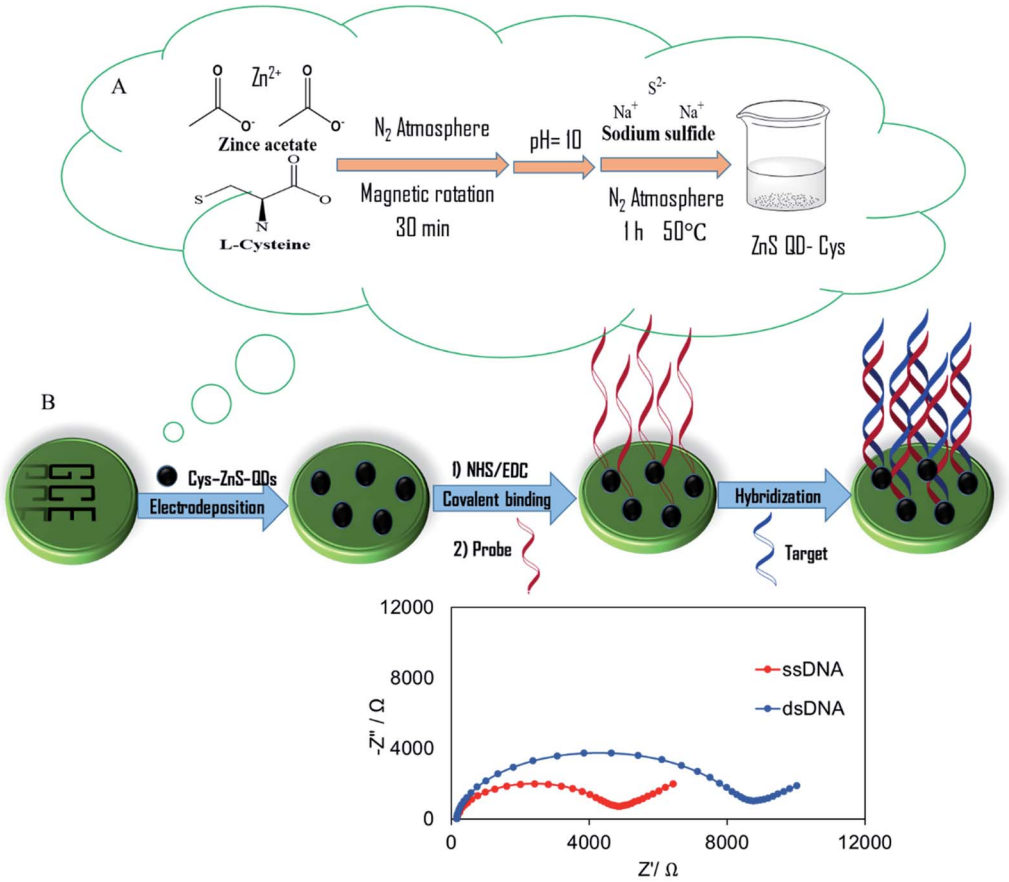

Scheme 1 Schematic representation of (A) the synthesis of L-cysteine functionalized ZnS-QDs and (B) the label free electrochemical genosensor fabrication for detecting miRNA (miR-200a).

2.2 Synthesis of Cys–ZnS-QDs

In a three-necked flask, 25.0 mL of aqueous solution of L-cysteine (0.02 M) was added dropwise to 25.0 mL of aqueous solution of zinc acetate (0.02 M) under a N_2 atmosphere and stirred for 30 minutes by using a magnetic stirrer. Under the above conditions, the pH of the solution was also increased to 10 using NaOH solution. Then, 5 mL Na_2S (0.1 M) was added to the solution and stored at 50 °C under a N_2 atmosphere for approximately one hour. The obtained Cys–ZnS-QDs were precipitated with ethanol, separated by centrifuging at 15 000 rpm, and finally washed with ethanol three times and allowed to dry in an oven at 60 °C for 12 hours.[30] The preparation method of Cys–ZnS-QDs is shown in Scheme 1A.

2.3 Preparation of the label-free genosensor to detect miR-200a

The preparation of the genosensor is illustrated in Scheme 1B. First, a GCE was polished with a 0.05 μm alumina–water slurry using a polishing cloth to obtain a smooth surface. The electrode surface was then cleaned by sonication in water and ethanol. Subsequently, the bare GCE was placed in a Cys–ZnS-QD solution and the potential was scanned in the range of −0.8 to +2.0 V at a scan rate of 100.0 mV s^{-1} for seven cycles to electrodeposit Cys–ZnS-QDs on the electrode surface (Cys–ZnS-QD/GCE) and then it was washed with phosphate buffer (0.1 M, pH 7.0).[33] The carboxyl groups of Cys–ZnS-QDs were activated by placing the modified electrode in a 1 : 1 solution of EDC (0.4 M) and NHS (0.1 M) solution for 45 min.

In the next step, 2.5 μL NH_2-probe (ssDNA) solution was placed on the surface of the modified electrode and held in a humid environment for 90.0 minutes. The $-NH_2$ groups in the amino modified ssDNA form strong covalent bonds (C–N) with –COOH groups of Cys–ZnS-QDs to immobilize the probe on the surface of the Cys–ZnS-QDs/GCE. The unbounded ssDNA was removed by rinsing the modified electrode with phosphate buffer (0.1 M, pH 7.0). Finally, the hybridization process was implemented by placing 5.0 μL of the target (complementary, single-base mismatch or non-complementary) solution onto the ssDNA/Cys–ZnS-QD/GCE surface, followed by incubation in a humid container at room temperature for 90.0 minutes. The electrode was then rinsed with phosphate buffer (0.1 M, pH 7.0) to remove excess oligonucleotides.

3. Results and discussion

3.1 Characterization of L-cysteine modified ZnS-QDs

TEM was used to determine the particle size of the Cys–ZnS-QDs. Fig. 1A and B show the TEM image and the distribution

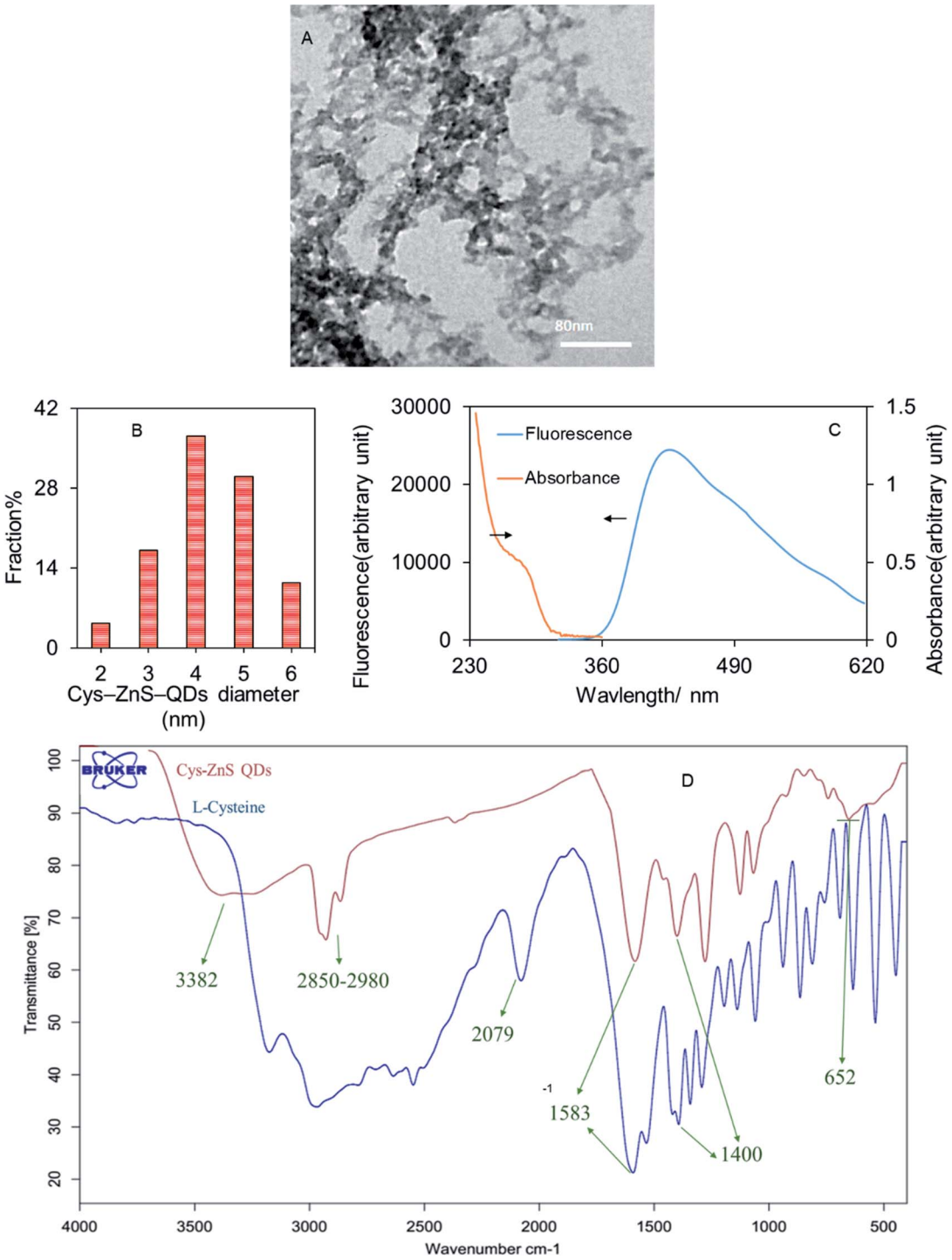

Fig. 1 (A) TEM image (B) distribution histogram and (C) absorption and fluorescence spectra of Cys–ZnS-QDs. (D) FT-IR spectra of the Cys–ZnS-QDs and L-Cysteine.

histogram of the size of the Cys–ZnS-QDs, respectively. The distribution histogram was drawn based on the data of the TEM image. Based on the distribution histogram, the size of the Cys–ZnS-QDs in the aqueous solution was found to be 2 to 6 nm, and its average size was estimated to be 4.3 ± 0.9 nm. L-Cysteine functionalized ZnS-QDs were optically characterized by UV-Vis absorption and fluorometry. Fig. 1C shows the absorption and fluorescence emission spectra of the Cys–ZnS-QDs. The absorption and emission peaks at wavelengths of 250 and 420 nm represent the quantum dot energy bandgap, which depends on the size of QDs. In fact, as the size of QDs becomes smaller, the energy gap increases and hence the fluorescence wavelength becomes smaller.[34] Fig. 1D shows the FT-IR spectrum of L-cysteine and Cys–ZnS-QDs. The strong absorption

bands around 1583 and 1400 cm^{-1} in both spectra are attributed to the $-COO^-$ groups. Also, the absorption bands around 3382 cm^{-1} and 652 cm^{-1} are ascribed to the $-NH_2$ and C–S groups in both spectra. The absorption peak at about 2079 cm^{-1} in the L-cysteine spectrum belongs to the thiol group of L-cysteine. The loss of this absorption peak in the Cys–ZnS-QDs spectrum is due to the binding of the L-cysteine thiol group to ZnS-QDs and the formation of the S–S bond.[30] These results confirm that the ZnS-QDs were well-functionalized with L-cysteine. Also, the results of the Cys–ZnS-QD optical spectrum confirm the TEM results.

3.2 Electrochemical monitoring of the electrode surface during the modification steps

The electrochemical impedance spectroscopy (EIS), as the method, and $[Fe(CN)_6]^{3-/4-}$, as the redox probe, were used to monitor the genosensor preparation steps. The EIS spectra are in the form of Nyquist plots consisting of a semicircle in which the diameter represents the charge transfer resistance (R_{ct}) and the linear part represents a diffusion-limited process.[18] The Nyquist plots of the genosensor at different stages of its construction are shown in Fig. 2. Also, the components of the equivalent circuit corresponding to the Nyquist plots are shown in the inset of Fig. 2 and its details are described in Section S1 and Fig. S1 of the ESI.† As can be seen, the bare GCE exhibits a small R_{ct} (plot a), but the R_{ct} value increased for the modified electrode with Cys–ZnS-QDs due to the semiconductor properties of Cys–ZnS-QDs and the negative charge of the functional groups on Cys–ZnS-QDs prevents the redox probe from reaching the electrode surface (plot b). After immobilization of the NH_2-probe on the modified electrode surface, R_{ct} increased due to the repulsive effect between the negative charge of the ssDNA and $[Fe(CN)_6]^{3-/4-}$ probe (plot c). Finally, miR-200a was incubated on the ssDNA/Cys–ZnS-QD/GCE and hybridized with ssDNA, and R_{ct} continuously increased (plot d). This is related to the formation of dsDNA, which increases the density of the negative charges at the electrode surface. The results of fitting the Randles circuit corresponding to the Nyquist plots are shown in Table S1.†

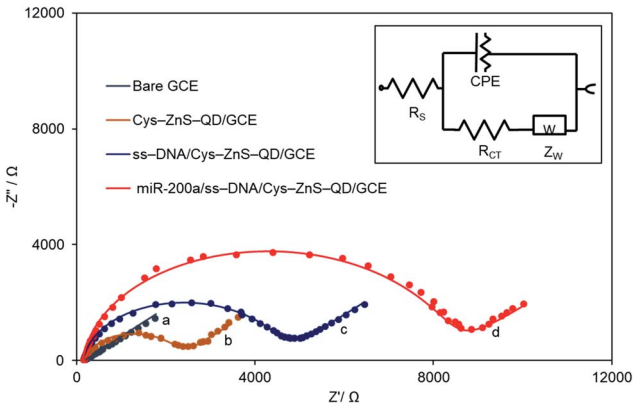

Fig. 2 Nyquist plots of (a) bare GCE, (b) Cys–ZnS-QD/GCE, (c) ssDNA/Cys–ZnS-QD/GCE and (d) ssDNA/Cys–ZnS-QD/GCE hybridized with 1.0×10^{-6} M of miR-200a in 0.1 M phosphate buffer (pH 7.0) containing 5.0 mM $[Fe(CN)6]^{3-/4-}$ and 0.1 M KCl.

3.3 Optimization of the experimental conditions

In order to obtain a sensitive and stable genosensor to determine miR-200a, the effective parameters such as its efficiency in the manufacturing process including probe concentration, probe immobilization time and hybridization time were optimized for three repeated measurements ($n = 3$). To optimize the probe concentration, different concentrations of the NH_2-probe (*i.e.* 4.0, 6.0, 8.0, 10.0, 12.0 and 14.0 μM) were immobilized on the Cys–ZnS-QD modified electrode after activation of carboxylic groups by using NHS/EDC. The probe immobilization time was 180 minutes. To hybridize the target, miR-200a (1.0 μM) was placed on the modified electrode surface for 120 minutes. The Nyquist plots were recorded after each step, and the difference between the R_{ct} values of the immobilized probe (ssDNA) on the modified electrode surface and that after hybridization with complementary DNA (dsDNA), $\Delta R_{ct} = R_{ct}(dsDNA) - R_{ct}(ssDNA)$, was accepted as the measurement signal. As shown in Fig. 3A, ΔR_{ct} increased with increasing concentration up to about 10.0 μM and then it remained almost constant. Therefore, 10.0 μM was selected as the optimum concentration of the NH_2-probe. The influence of the probe immobilization time on the surface of the modified electrode was also investigated. To find the optimum immobilization time of the probe, the modified electrode was incubated in a 10.0 μM NH_2-probe for 30.0, 60.0, 90.0, 120 and 180.0 minutes. The hybridization process was then performed by placing 1.0 μM miR-200a on the probe-modified electrode surface for 120 minutes. According to Fig. 3B, the highest ΔR_{ct} is obtained for a probe immobilization time of 90 minutes. Thus, 90 minutes was chosen as the optimum time to immobilize the NH_2-probe on the modified electrode surface. The decrease of the ΔR_{ct} value after 90 minutes is due to the excessive and inappropriate aggregation of oligonucleotides at the electrode surface leading to irregularities in the position, immobilization and inadequate access of the electroactive species on the electrode surface. The other effective parameter for the genosensor response is the hybridization time. To optimize the hybridization time, the probe (10.0 μM) was immobilized on the electrode surface for 90 minutes. Then, the ssDNA/Cys–ZnS-QD/GCE was incubated with 1.0 μM miR-200a for different times of 30.0, 60.0, 90.0, 120.0 and 180.0 minutes. Fig. 3C indicates the variations of the ΔR_{ct} value *versus* the hybridization time at the miR-200a/ssDNA/Cys–ZnS-QD/GCE surface. As expected, the amount of ΔR_{ct} increased with increasing hybridization time and reached a constant value in about 90 minutes and thus, this time was suggested as the optimum hybridization time.

3.4 Analytical performance of the label free genosensor for measuring miR-200a

The analytical performance of the genosensor was evaluated by measuring the EIS response dependent on the miR-200a concentration (1.0×10^{-14} to 1.0×10^{-6} M). Each measurement was repeated three times ($n = 3$). As shown in Fig. 4, the

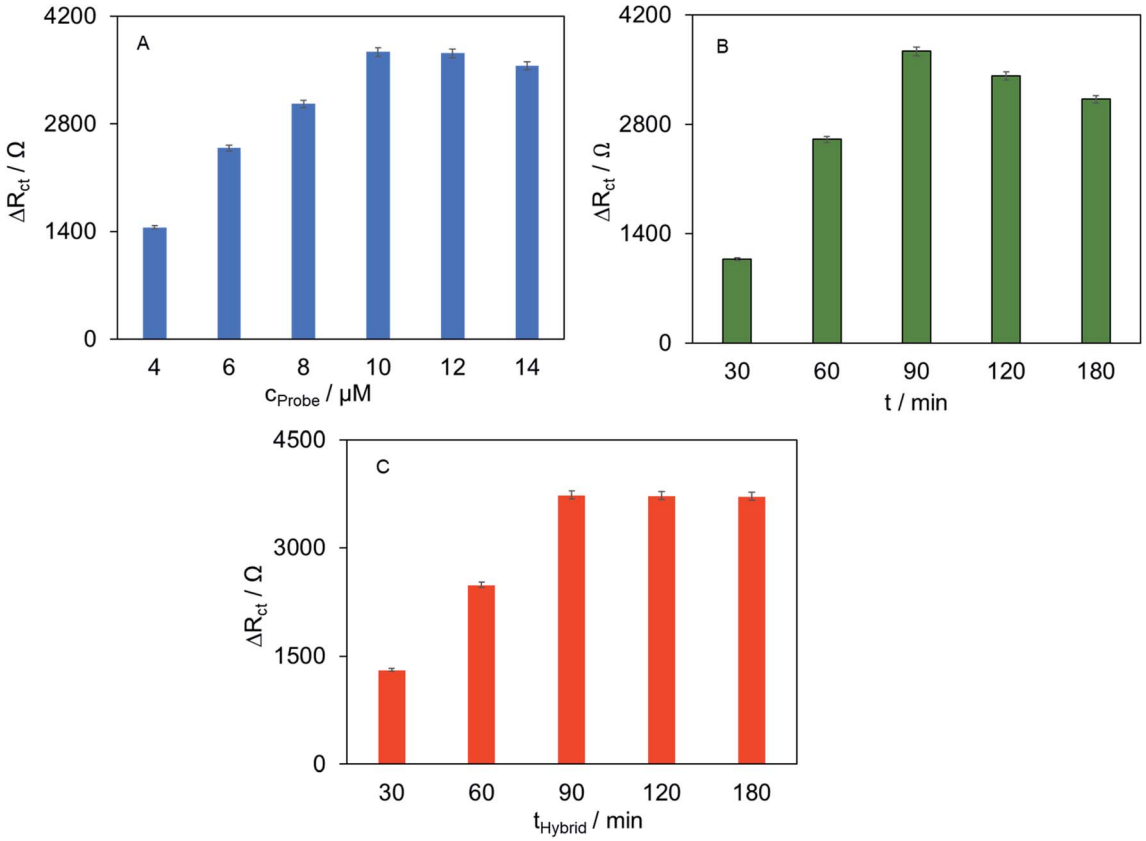

Fig. 3 Optimization of the ΔR_{ct} response ([miR-200a] = 1.0×10^{-6} M in all the experiments) by making variation in (A) concentrations of the NH_2-probe (probe immobilization time: 180 minutes and hybridization time: 120 minutes), (B) immobilization time of the NH_2-probe (probe concentration: 1.0×10^{-5} M and hybridization time: 120 minutes) and (C) hybridization time (probe concentration: 1.0×10^{-5} M and probe immobilization time: 90 minutes) during the fabrication of the electrochemical genosensor. Error bars correspond to the relative standard deviation of three repeated measurements ($n = 3$).

semicircle diameter of the Nyquist plots increased with increase in the miR-200a concentration. The inset A of Fig. 4 shows the calibration plots for the quantitative determination of miR-200a. The change of the R_{ct} value before, R_{ct}(ssDNA), and after hybridization with miR-200a, R_{ct}(dsDNA), was calculated for each miR-200a concentration and used as the analytical response. As illustrated from the inset A of Fig. 4, there was a linear dependence between the ΔR_{ct} value and the logarithmic concentration of miR-200a in the concentration range 1.0×10^{-14} to 1.0×10^{-6} M. Using the calibration plot slope of Fig. 4, inset A, and the equation $y_{LOD} = y_b + 3S_b$, a value of 8.4 fM was obtained for the detection limit of miR-200a. In this equation, y_b and S_b represent the analytical response and the standard deviation of the blank solution, respectively.[35] The Randles equivalent circuit which was used as an equivalent circuit model to fit the impedance data is shown in inset B of Fig. 4. Also, Table S2† shows the results of fitting based on the Randles circuit. The performance of the genosensor to determine miR-200a was evaluated by comparing some of the analytical parameters of this genosensor and those of other published papers (Table 1). The results show that the analytical parameters of the proposed genosensor are better in some cases or comparable to those reported in the literature. As can be seen from the results of Table 1, the linear concentration range of the proposed genosensor are wider than those reported by others. Also, the detection limit of the genosensor is lower than most reports that have been published in this regard. In addition, the sensitivity is comparable to those of other genosensors.

3.5 Selectivity, stability, reproducibility, and repeatability of the label free genosensor

The EIS method was used to evaluate the selectivity of the genosensor to detect miR-200a (complementary) from a non-complementary and one-base mismatch target sequences. For this purpose, the ssDNA/Cys–ZnS-QD/GCE was hybridized with two concentrations of 1.0×10^{-6} M and 1.0×10^{-11} M of miR-200a, non-complementary and one-base mismatch sequences. The corresponding Nyquist plots are shown in Fig. 5A and S2.† The ΔR_{ct} responses for three repeated measurements ($n = 3$) induced by different target DNA sequences are also displayed in Fig. 5B. As can be seen, when ssDNA/Cys–ZnS-QD/GCE hybridization is performed with the complementary sequence, the largest electrochemical response (ΔR_{ct}) is obtained compared to the hybridization with one-base mismatch target and non-complementary sequences. The results show that only the

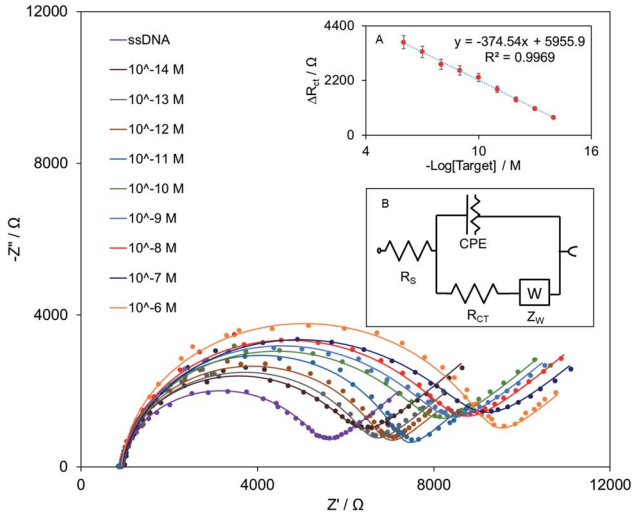

Fig. 4 Nyquist plots recorded at the ssDNA/Cys–ZnS-QD/GCE surface after hybridization with different concentrations of miR-200a in 0.1 M phosphate buffer (pH 7.0) containing 5.0 mM $[Fe(CN)_6]^{3-/4-}$ and 0.1 M KCl. Insets: (A) a calibration plot of the changes in the electron transfer resistance, $\Delta R_{ct} = R_{ct}(dsDNA) - R_{ct}(ssDNA)$, *vs.* log [miR-200a] and (B) the Randles equivalent circuit to fit the EIS data. Error bars correspond to the relative standard deviation of three repeated measurements ($n = 3$).

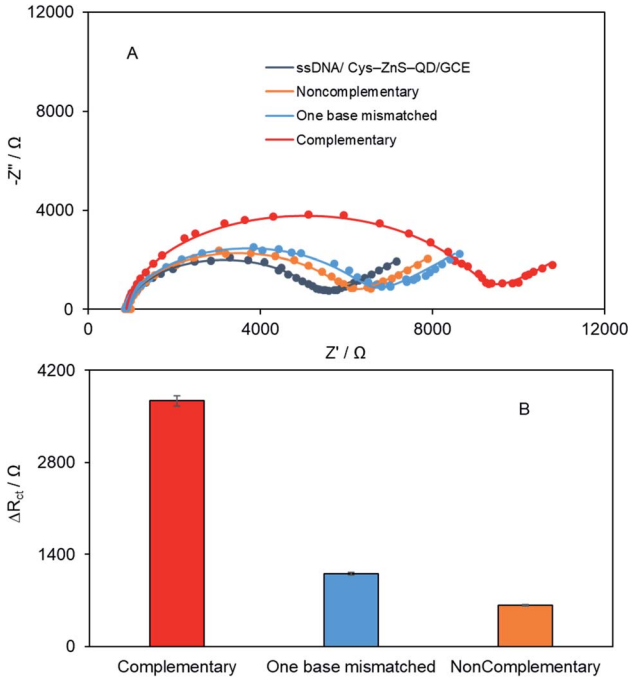

Fig. 5 (A) Nyquist plots of the ssDNA/Cys–ZnS-QD/GCE before and after hybridization with 1.0×10^{-6} M miR-200a (as a complementary sequence), one-base mismatch and noncomplementary sequence in 0.1 M phosphate buffer (pH 7.0) containing 5.0 mM $[Fe(CN)_6]^{3-/4-}$ and 0.1 M KCl. (B) The ΔR_{ct} responses for three repeated measurements ($n = 3$) induced by different target DNA sequences (miR-200a, noncomplementary and one-base mismatch).

complementary sequence is completely hybridized with the ssDNA/Cys–ZnS-QD/GCE and the hybridization process is complete only in the presence of miR-200a. In addition, the difference in the response of the complementary and the one-base mismatch indicates high selectivity of the genosensor to detect miR-200a. The stability of the label free genosensor was evaluated by storing the ssDNA/Cys–ZnS-QDs/GCE at 4 °C for two days. The response of the genosensor for 1.0×10^{-12} M miR-200a was about 93% of its initial response and the relative standard deviation of the response was 3.7%. In order to test the

Table 1 Comparison of some analytical parameters of various biosensors used to determine miRNA-200a and the other miRNAs[a]

Method[b]	miRNA	Recognition element or redox mediator	Linear range/M	Detection limit/fM	Sensitivity	Reference
EIS	miR-25	$[Fe(CN)6]^{3-/4-}$	1.0×10^{-12}–1.0×10^{-10}, 1.0×10^{-10}–1.0×10^{-6}	250	1.7638, 0.9444 KΩ M^{-1}	1
CV	miR-182	Bioten-miRNA	1.0×10^{-13}–1.0×10^{-11}	10	−0.706 μA pM^{-1}	37
CV	miR-155	Nafion/thionine	5.6×10^{-12}–5.6×10^{-7}	1870	1.7281 μA pM^{-1}	38
DPV	miR-21	Hemin	1.0×10^{-14}–5.0×10^{-10}	6	0.4301 μA pM^{-1}	39
DPV	miR-155	Oracet blue	5.0×10^{-11}–15×10^{-9}	13500	−22.296 nA nM^{-1}	40
DPV	miR-24	Oxidation of guanine	1.0×10^{-12}–1.0×10^{-9}, 1.0×10^{-9}–1.0×10^{-8}	1000	0.2822, 4.963 μA per cm^2 per decade	41
DPV	miR-21	Methylene blue	1.0×10^{-13}–5.0×10^{-10}	84.3	1.51 μA/M	42
EIS	miR-125a	$[Fe(CN)6]^{3-/4-}$	1.0×10^{-9}–2.0×10^{-6}	1.0×10^4	83.39 Ω M^{-1}	43
EIS	miR-200a	$[Fe(CN)6]^{3-/4-}$	1.0×10^{-14}–1.0×10^{-6}	8.4	374.54 Ω M^{-1}	This work

[a] Cys-AuNPs/GCE: cysteamine-capped gold nanoparticles/glassy carbon electrode, nano-Pd/GCE: Pd nanoparticles/glass carbon electrode, AuNPs/Au-E: gold nanoparticles/gold electrode, thiolated CP/Au-E: thiolated single strand capture probe/gold electrode, MWCNTs/GCE: MWCNT modified glass carbon electrode, MWCNTs-COOH/GCE: carboxylated MWCNT modified glass carbon electrode, FC-AuNPs/AuE: Fc-capped gold nanoparticle/gold electrode, Cys–ZnS-QD/GCE: L-cysteine functionalized ZnS quantum dots/glass carbon electrode, and PGE/CB: pencil graphite electrode/carbon black. [b] EIS: electrochemical impedance spectroscopy, DPV: differential pulse voltammetry, CV: cyclic voltammetry.

Table 2 Results of the relative standard deviations and recovery rates of miR-200a in a human blood plasma sample ($n = 3$) by the proposed genosensor

Sample	Added/M	Found/M	Recovery (%)	RSD (%)
Blood plasma	1.0×10^{-12}	9.4×10^{-13}	94.0	2.5
	5.0×10^{-12}	5.2×10^{-12}	104.0	3.0
	1.0×10^{-11}	9.6×10^{-12}	96.0	4.1

reproducibility of the label free genosensor, three ssDNA/Cys–ZnS-QDs/GCE were prepared on different days and a concentration of 1.0×10^{-12} M miR-200a was incubated on them. The Nyquist plots were then recorded and their ΔR_{ct} values were calculated. The average response and the relative standard deviation (RSD) for the repeated measurements of miR-200a were found to be 1422.8 ± 93.2 Ω and 6.5%, respectively. The repeatability of the label free genosensor was also evaluated for the concentration of 1.0×10^{-12} M miR-200a in 10 repeated measurements. The average response and the relative standard deviation (RSD) were found to be 1414.9 ± 56.1 Ω and 4.0%, respectively. The results demonstrate the acceptable reproducibility and repeatability of the label free genosensor.

3.6 Determination of miR-200a in blood plasma samples

Due to the important role of early detection in cancer treatment, the proposed genosensor was used for the quantitative analysis of miR-200a, an ovarian cancer biomarker, in blood plasma samples. Usually the miRNA concentration in many biological samples is not sufficient to assay miRNA because circulating miRNAs are present at femtomolar concentrations or even lower levels in the blood.[36,37] Since the concentration of miR-200a in the plasma of healthy individuals is less than the detection limit of the proposed genosensor,[1] the initial concentration of miR-200a in the plasma sample is assumed to be zero. In order to measure miR-200a in a plasma sample, 10.0 μL of the healthy plasma sample was diluted to 100.0 μL with the hybridization buffer solution. In the next step, appropriate amounts of miR-200a were spiked to the diluted plasma sample and the recovery rates were estimated by the EIS method. The calibration plot in the concentration range of 1.0×10^{-14} to 1.0×10^{-6} M was used to analyse the blood plasma sample. The results are summarized in Table 2. As deduced from Table 2, the relative standard deviations (RSD%) and the recovery rates of the spiked samples were acceptable. The proposed genosensor can therefore be potentially used to monitor miR-200a in a complex biological sample such as plasma.

4. Conclusion

In the present study, an electrochemical genosensor based on L-cysteine functionalized ZnS quantum dots was introduced to determine miRNA-200a, a biomarker of ovarian cancer. The synthesized L-cysteine functionalized ZnS quantum dots provide an increase in active sites that leads to easier capture of the probe by NHS/EDC as an activator on the GCE surface. Using EIS, the analytical performance of this genosensor to measure miR-200a was investigated and a concentration range of 1.0×10^{-14} to 1.0×10^{-6} M and detection limit of 8.4 fM were obtained. The genosensor is selective and can be used to detect miR-200a from a one-base mismatch sequence. Moreover, the label free genosensor is able to detect miR-200a in human blood plasma without requiring sample pretreatment.

Conflicts of interest

There are no conflicts to declare.

References

1 A. Asadzadeh-Firouzabadi and H. R. Zare, *Anal. Methods*, 2017, **9**, 3852–3861.
2 Y. Zhang, Y. Yan, W. Chen, W. Cheng, S. Li, X. Ding, D. Li, H. Wang, H. Ju and S. Ding, *Biosens. Bioelectron.*, 2015, **68**, 343–349.
3 C. Glinge, S. Clauss, K. Boddum, R. Jabbari, J. Jabbari, B. Risgaard, P. Tomsits, B. Hildebrand, S. Kääb and R. Wakili, *PLoS One*, 2017, **12**, e0167969.
4 A. Pendlebury, N. J. Hannan, N. Binder, S. Beard, M. Mcgauran, P. Grant, S. Tong and C. L. Whitehead, *Biomed. Rep.*, 2017, **6**, 319–322.
5 H. Yin, Y. Zhou, H. Zhang, X. Meng and S. Ai, *Biosens. Bioelectron.*, 2012, **33**, 247–253.
6 M. Koutsaki, M. Libra, D. A. Spandidos and A. Zaravinos, *Oncotarget*, 2017, **8**, 66629.
7 G. C. Jayson, E. C. Kohn, H. C. Kitchener and J. A. Ledermann, *Lancet*, 2014, **384**, 1376–1388.
8 E. Gov, M. Kori and K. Y. Arga, *Syst. Biol. Reprod. Med.*, 2017, **63**, 219–238.
9 G. Muralidhar and M. Barbolina, *Int. J. Mol. Sci.*, 2015, **16**, 16833–16847.
10 P.-W. Choi, A. Bahrampour, S.-K. Ng, S. K. Liu, W. Qiu, F. Xie, W. P. Kuo, J. Kwong, K. H. Hales and D. B. Hales, *Sci. Rep.*, 2020, **10**, 1–9.
11 M. Zuberi, R. Mir, J. Das, I. Ahmad, J. Javid, P. Yadav, M. Masroor, S. Ahmad, P. Ray and A. Saxena, *Clin. Transl. Oncol.*, 2015, **17**, 779–787.
12 B. Li, F. Liu, Y. Peng, Y. Zhou, W. Fan, H. Yin, S. Ai and X. Zhang, *Biosens. Bioelectron.*, 2016, **79**, 307–312.
13 Z. Czimmerer, J. Hulvely, Z. Simandi, E. Varallyay, Z. Havelda, E. Szabo, A. Varga, B. Dezso, M. Balogh and A. Horvath, *PLoS One*, 2013, **8**, e55168.
14 X.-J. Lu and W. K. Olson, *Nat. Protoc.*, 2008, **3**, 1213.
15 F. Porichis, M. G. Hart, M. Griesbeck, H. L. Everett, M. Hassan, A. E. Baxter, M. Lindqvist, S. M. Miller, D. Z. Soghoian and D. G. Kavanagh, *Nat. Commun.*, 2014, **5**, 1–12.
16 M. Daneshpour, K. Omidfar and H. Ghanbarian, *Beilstein J. Nanotechnol.*, 2016, **7**, 2023–2036.
17 X. Lu, H. Zhang, Y. Ni, Q. Zhang and J. Chen, *Biosens. Bioelectron.*, 2008, **24**, 93–98.
18 I. I. Suni, *Trends in Analytical Chemistry*, 2008, **27**, 604–611.

19 A. Asadzadeh-Firouzabadi and H. R. Zare, *J. Electrochem. Soc.*, 2017, **164**, B1–B9.
20 N. Nasirizadeh, H. R. Zare, M. H. Pournaghi-Azar and M. S. Hejazi, *Biosens. Bioelectron.*, 2011, **26**, 2638–2644.
21 A. Asadzadeh-Firouzabadi and H. R. Zare, *Sens. Actuators, B*, 2018, **260**, 824–831.
22 A. Akbarnia and H. R. Zare, *Microchim. Acta*, 2018, **185**, 503.
23 Z. Shekari, H. R. Zare and A. Falahati, *Anal. Biochem.*, 2017, **518**, 102–109.
24 Z. Shekari, H. R. Zare and A. Falahati, *Microchim. Acta*, 2019, **186**, 530.
25 Y. Zhang and Q. Wei, *J. Electroanal. Chem.*, 2016, **781**, 401–409.
26 S. N. Topkaya, M. Azimzadeh and M. Ozsoz, *Electroanalysis*, 2016, **28**, 1402–1419.
27 J. Mal, Y. Nancharaiah, E. Van Hullebusch and P. Lens, *RSC Adv.*, 2016, **6**, 41477–41495.
28 F. Zhang, C. Li, X. Li, X. Wang, Q. Wan, Y. Xian, L. Jin and K. Yamamoto, *Talanta*, 2006, **68**, 1353–1358.
29 A. Sharma, V. K. Rao, D. V. Kamboj, R. Gaur, S. Upadhyay and M. Shaik, *Biotechnology Reports*, 2015, **6**, 129–136.
30 G. Hosseinzadeh, A. Maghari, S. M. F. Farniya, A. H. Keihan and A. A. Moosavi-Movahedi, *Materials Science and Engineering C*, 2017, **77**, 836–845.
31 F. Lisdat and D. Schäfer, *Anal. Bioanal. Chem.*, 2008, **391**, 1555.
32 S. Pan and L. Rothberg, *Langmuir*, 2005, **21**, 1022–1027.
33 O. K. Y. Sahin, *Int. J. Electrochem. Sci.*, 2018, **13**, 159–174.
34 M. F. Frasco and N. Chaniotakis, *Sensors*, 2009, **9**, 7266–7286.
35 J. Miller and J. C. Miller, *Statistics and chemometrics for analytical chemistry*, Pearson education, 2018.
36 P. S. Mitchell, R. K. Parkin, E. M. Kroh, B. R. Fritz, S. K. Wyman, E. L. Pogosova-Agadjanyan, A. Peterson, J. Noteboom, K. C. O'Briant and A. Allen, *Proc. Natl. Acad. Sci. U. S. A.*, 2008, **105**, 10513–10518.
37 J. Wang, X. Yi, H. Tang, H. Han, M. Wu and F. Zhou, *Anal. Chem.*, 2012, **84**, 6400–6406.
38 X. Wu, Y. Chai, R. Yuan, H. Su and J. Han, *Analyst*, 2013, **138**, 1060–1066.
39 X. Meng, Y. Zhou, Q. Liang, X. Qu, Q. Yang, H. Yin and S. Ai, *Analyst*, 2013, **138**, 3409–3415.
40 M. Azimzadeh, M. Rahaie, N. Nasirizadeh and H. Naderi-Manesh, *Anal. Methods*, 2015, **7**, 9495–9503.
41 F. Li, J. Peng, J. Wang, H. Tang, L. Tan, Q. Xie and S. Yao, *Biosens. Bioelectron.*, 2014, **54**, 158–164.
42 H.-A. Rafiee-Pour, M. Behpour and M. Keshavarz, *Biosens. Bioelectron.*, 2016, **77**, 202–207.
43 G. Yammouri, J. Mandli, H. Mohammadi and A. Amine, *J. Electroanal. Chem.*, 2017, **806**, 75–81.